DALTON

# Deprotonation of the carbaborane *nido*-7-$NH_2Bu^t$-7-$CB_{10}H_{12}$: crystal structures of *nido*-7-$NH_2Bu^t$-7-$CB_{10}H_{12}$ and [$NEt_3(CH_2Ph)$]-[*nido*-7-$NHBu^t$-7-$CB_{10}H_{12}$]

**John C. Jeffery,[a] Paul A. Jelliss,[b] James Karban,[b] Vyacheslav Lebedev[b] and F. Gordon A. Stone*[,b]**

[a] *School of Chemistry, The University of Bristol, Bristol BS8 1TS, UK*
[b] *Department of Chemistry, Baylor University, Waco, TX 76798–7348, USA*

The crystal structure of *nido*-7-$NH_2Bu^t$-7-$CB_{10}H_{12}$ **1** has been determined by X-ray diffraction. The compound crystallises in the orthorhombic space group *Pbca* [$a$ = 10.507(5), $b$ = 13.805(6), $c$ = 18.093(9) Å]. The *nido*-icosahedral structure was established with two *endo*-B–H–B and two $NH_2$ hydrogen atoms located in Fourier-difference maps and refined. The structure determination is also supported by $^{11}$B-{$^1$H}–$^{11}$B-{$^1$H} correlation NMR spectroscopy. A molecular orbital calculation and frontier density analysis of **1** indicated that deprotonation should initially occur at the *exo*-nitrogen atom. Treatment of **1** with 1 equivalent of $LiBu^n$, followed by addition of [$NEt_3(CH_2Ph)$]Cl, gave [$NEt_3(CH_2Ph)$][*nido*-7-$NHBu^t$-7-$CB_{10}H_{12}$] **2** as the only product and single crystals were grown for an X-ray diffraction study. The salt crystallises in the monoclinic space group $P2_1/n$ [$a$ = 10.651(2), $b$ = 11.652(2), $c$ = 20.926(3) Å, β = 101.77(2)°]. The $^1$H, $^{13}$C-{$^1$H} and $^{11}$B-{$^1$H} NMR spectra of **1** and **2** have also been recorded.

We have recently shown that the zwitterionic monocarbaborane *nido*-7-$NH_2Bu^t$-7-$CB_{10}H_{12}$ **1**, first reported by Todd and co-workers,[1] is a useful precursor for the synthesis of ruthena-, osma- and rhoda-carbaboranes in direct reactions with low-valent compounds of these metals.[2] During studies with [RhX-($PPh_3$)$_3$] (X = Cl or Br) as a precursor it was observed that some of the initially formed species containing the Rh(η$^5$-7-$NH_2Bu^t$-7-$CB_{10}H_{10}$) fragment subsequently deprotonated to give complexes with Rh(η$^5$-7-$NHBu^t$-7-$CB_{10}H_{10}$) groups. In other reactions complexes with the Rh(η$^5$-7-$NHBu^t$-7-$CB_{10}H_{10}$) moiety were formed directly from the *nido*-carbaborane. Whereas the charge-compensated η$^5$-7-$NH_2Bu^t$-7-$CB_{10}H_{10}$ ligand is formally a four-electron donor, the η$^5$-7-$NHBu^t$-$CB_{10}H_{10}$ unit is formally a three-electron donor. These transformations prompted studies of the reagent **1** itself.

## Results and Discussion

Spectroscopic and structural data for *nido*-7-$NH_2Bu^t$-7-$CB_{10}H_{12}$ **1** are lacking and so the NMR spectra were recorded and an X-ray diffraction study was carried out. The $^1$H NMR spectrum displayed one broad resonance at δ −3.62 for the equivalent *endo*-B–H–B protons, and resonances at δ 1.56 for the $Bu^t$ group and at δ 7.72 for the $NH_2$ fragment, the latter also being broad. As expected the three peaks were of relative intensity 2:9:2, respectively. The chemical shift of the $NH_2$ protons is in the range found for complexes containing a Rh(η$^5$-7-$NH_2Bu^t$-7-$CB_{10}H_{10}$) unit.[2b] The $^{13}$C-{$^1$H} NMR spectrum had a diagnostic peak for the cage-carbon nucleus at δ 93.1 and resonances for the $Bu^t$ group were seen at δ 64.1 ($CMe_3$) and 28.0 ($CMe_3$). Discussion of the $^{11}$B-{$^1$H} NMR spectrum is deferred until after the results of the X-ray diffraction have been reported.

Selected internuclear distances and angles for compound **1** are listed in Table 1 and the molecular structure is shown in Fig. 1. The *nido* structure is clearly revealed with the $NH_2Bu^t$ substituent attached to carbon C(1) in the open face of the cage. The bridging hydrogen atoms H(23) and H(45), spanning the connectivities B(2)–B(3) and B(4)–B(5) respectively, were located from final electron-density difference syntheses as were the hydrogens H(1A) and H(1B) attached to N. As can be seen in Fig. 1 a molecular plane of symmetry including the atoms

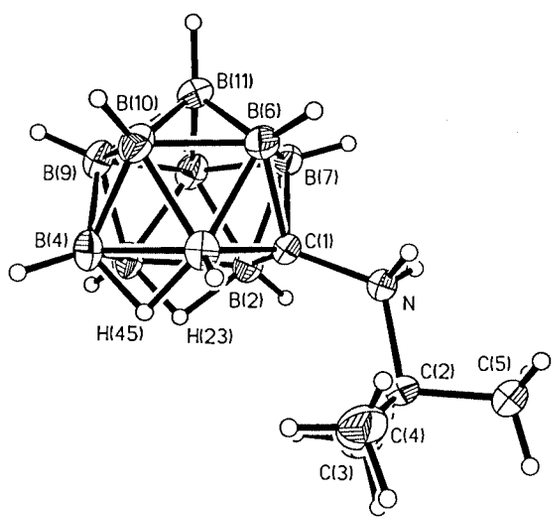


**Fig. 1** Molecular structure of *nido*-7-$NH_2Bu^t$-7-$CB_{10}H_{12}$ **1** showing the atom labelling scheme. Ellipsoids are drawn at the 40% probability level

B(9), C(1), N, C(2) and C(5) can be readily generated in solution in agreement with the observed NMR data.

The $^{11}$B-{$^1$H} NMR spectrum of compound **1** displayed a set of six peaks (1:2:2:2:1:2), consistent with the above-mentioned plane of symmetry. The $^{11}$B-{$^1$H}–$^{11}$B-{$^1$H} correlation spectroscopy (COSY) NMR spectrum (Fig. 2) confirms that the solid-state structure, determined by the single-crystal X-ray diffraction study, is maintained in solution with the obvious additional degrees of rotational freedom about bonds in the $NH_2Bu^t$ group. The connectivity map emphasises the mirror symmetry of the *nido*-carbaborane and a unique set of predicted and observed $^{11}$B–$^{11}$B correlations is shown by the solid lines. As expected, $^{11}$B–$^{11}$B correlation is not observed between chemically equivalent boron atoms or for those boron atoms which are bridged by the *endo*-H hydrogen atoms.[3] The resulting pattern of $^{11}$B–$^{11}$B connectivities uniquely determines the *nido*-icosahedral structure of **1** in solution and allows a complete assignment (Experimental section) of the chemical shifts of the boron nuclei in the molecule. A significant reduction in

**Table 1** Selected internuclear distances (Å) and angles (°) for *nido*-7-$NH_2Bu^t$-7-$CB_{10}H_{12}$ **1** with estimated standard deviations in parentheses

| | | | | | | | |
|---|---|---|---|---|---|---|---|
| N–C(1) | 1.508(2) | N–C(2) | 1.553(2) | N–H(1A) | 0.93(2) | N–H(1B) | 0.93(2) |
| C(1)–B(2) | 1.653(3) | C(1)–B(5) | 1.655(3) | C(1)–B(7) | 1.698(3) | C(1)–B(6) | 1.707(3) |
| C(2)–C(4) | 1.512(3) | C(2)–C(3) | 1.514(3) | C(2)–C(5) | 1.518(3) | B(2)–B(8) | 1.788(3) |
| B(2)–B(7) | 1.813(3) | B(2)–B(3) | 1.854(3) | B(2)–H(23) | 1.34(2) | B(3)–B(9) | 1.756(3) |
| B(3)–B(8) | 1.774(3) | B(3)–B(4) | 1.881(3) | B(3)–H(23) | 1.22(2) | B(4)–B(9) | 1.750(3) |
| B(4)–B(10) | 1.775(3) | B(4)–B(5) | 1.856(3) | B(4)–H(45) | 1.24(2) | B(5)–B(10) | 1.785(3) |
| B(5)–B(6) | 1.812(3) | B(5)–H(45) | 1.34(2) | B(6)–B(7) | 1.744(3) | B(6)–B(11) | 1.751(3) |
| B(6)–B(10) | 1.762(3) | B(7)–B(11) | 1.748(3) | B(7)–B(8) | 1.761(3) | B(8)–B(9) | 1.788(3) |
| B(8)–B(11) | 1.796(3) | B(9)–B(11) | 1.769(3) | B(9)–B(10) | 1.781(3) | B(10)–B(11) | 1.795(3) |

| | | | | | |
|---|---|---|---|---|---|
| C(1)–N–C(2) | 122.1(1) | C(1)–N–H(1A) | 108(1) | C(2)–N–H(1A) | 106(1) |
| C(1)–N–H(1B) | 106(1) | C(2)–N–H(1B) | 108(1) | H(1A)–N–H(1B) | 106(2) |
| N–C(1)–B(2) | 118.2(1) | N–C(1)–B(5) | 120.1(1) | B(2)–C(1)–B(5) | 112.3(1) |
| N–C(1)–B(7) | 113.2(1) | B(2)–C(1)–B(7) | 65.5(1) | B(5)–C(1)–B(7) | 115.6(1) |
| N–C(1)–B(6) | 114.2(1) | B(2)–C(1)–B(6) | 115.8(1) | B(5)–C(1)–B(6) | 65.2(1) |
| B(7)–C(1)–B(6) | 61.6(1) | C(4)–C(2)–C(3) | 111.9(2) | C(4)–C(2)–C(5) | 110.5(2) |
| C(3)–C(2)–C(5) | 110.7(2) | C(4)–C(2)–N | 110.0(2) | C(3)–C(2)–N | 108.9(2) |
| C(5)–C(2)–N | 104.5(1) | | | | |

**Table 2** Calculated bond orders for the C–B and B–B cage connectivities in compound **1**

| | | | |
|---|---|---|---|
| C(1)–B(2) | 0.790 | B(5)–B(6) | 0.305 |
| C(1)–B(5) | 0.790 | B(5)–B(10) | 0.532 |
| C(1)–B(6) | 0.491 | B(6)–B(7) | 0.392 |
| C(1)–B(7) | 0.484 | B(6)–B(10) | 0.537 |
| B(2)–B(3) | 0.348 | B(6)–B(11) | 0.534 |
| B(2)–B(7) | 0.306 | B(7)–B(8) | 0.537 |
| B(2)–B(8) | 0.532 | B(7)–B(11) | 0.535 |
| B(3)–B(4) | 0.732 | B(8)–B(9) | 0.506 |
| B(3)–B(8) | 0.498 | B(8)–B(11) | 0.386 |
| B(3)–B(9) | 0.333 | B(9)–B(10) | 0.506 |
| B(4)–B(5) | 0.348 | B(9)–B(11) | 0.524 |
| B(4)–B(9) | 0.334 | B(10)–B(11) | 0.386 |
| B(4)–B(10) | 0.497 | | |

correlation is observed between boron nuclei B(2, 5) and B(6, 7) compared with the remaining signals. In the $^{11}B$-{$^1H$}–$^{11}B$-{$^1H$} COSY NMR spectrum of the monocarbaborane *arachno*-4-$CB_8H_{14}$,[4a] recently synthesized by a new method,[4b] a similar feature was noted for the B(1) ⟷ B(5, 9) peak and was attributed to a reduction in electron density within the B(1)–B(5) and B(1)–B(9) vectors, as a result of their location adjacent to the cage-carbon atom. In compound **1** the boron atoms B(2), B(5), B(6) and B(7) are all adjacent to the cage-carbon atom, and a similar effect is thus expected. As will be discussed shortly, compound **1** was the subject of a molecular orbital analysis by MOPAC[5] based on the X-ray structural parameters. The C–B and B–B bond orders for the cage in **1**, as calculated by MOPAC, are shown in Table 2. Among these, the bond orders of 0.306 and 0.305 for the B(2)–B(7) and B(5)–B(6) connectivities, respectively, are the lowest perceptible. Furthermore, the internuclear distances B(2)–B(7) and B(5)–B(6) [1.813(3) and 1.812(3) Å, respectively] are notably longer than the average (1.77 Å) of the remaining B–B distances. This latter distance does not include the three open-face B–B distances (average 1.86 Å), which are invariably found to be long (>1.80 Å) in similar *nido*-$C_nB_{11-n}$ ($n = 1$ or 2) structures.[6a] Therefore the depletion of electron density between the boron vertices B(2)–B(7) and B(5)–B(6) in **1** is verified.

The deprotonation of carbaboranes such as *nido*-7,8-$R_2$-7,8-$C_2B_9H_{11}$ (R = H or Me) with strong bases such as NaH and $LiBu^n$ to produce anionic species *nido*-7,8-$R_2$-7,8-$C_2B_9H_n^{m-}$ ($n = 10$, $m = 1$; $n = 9$, $m = 2$) is well documented,[6] and is important in the context of the synthesis of metallacarbaborane complexes.[7] The process of deprotonation involves successive removal of the two acidic *endo*-B–H–B protons, the terminal *exo*-B–H protons not being candidates for such abstraction by virtue of their hydridic nature. By introducing an exopolyhedral group to a carbaborane such as $NH_2Bu^t$ in compound **1** the question arises as to the site where the first proton will be removed upon addition of an equivalent of base, and what the structure of the resulting stable product will be. In part this question has been answered by Todd and co-workers[1] who converted the compound *nido*-7-$NH_2$Me-7-$CB_{10}H_{12}$ into *nido*-7-$NMe_3$-7-$CB_{10}H_{12}$ by deprotonating the former with NaH and then adding $SO_2(OMe)_2$. Here the exopolyhedral $NH_2$Me group must clearly proceed through a deprotonation/methylation sequence. However, little is known about the potential stability or exact nature of intermediate charged species. We wished to study compound **1** specifically and examine whether the result of monodeprotonation agreed with that predicted on the basis of a simple molecular orbital calculation, and whether the stability of the monodeprotonated product was in keeping with results from our rhodacarbaborane work.[2b,c]

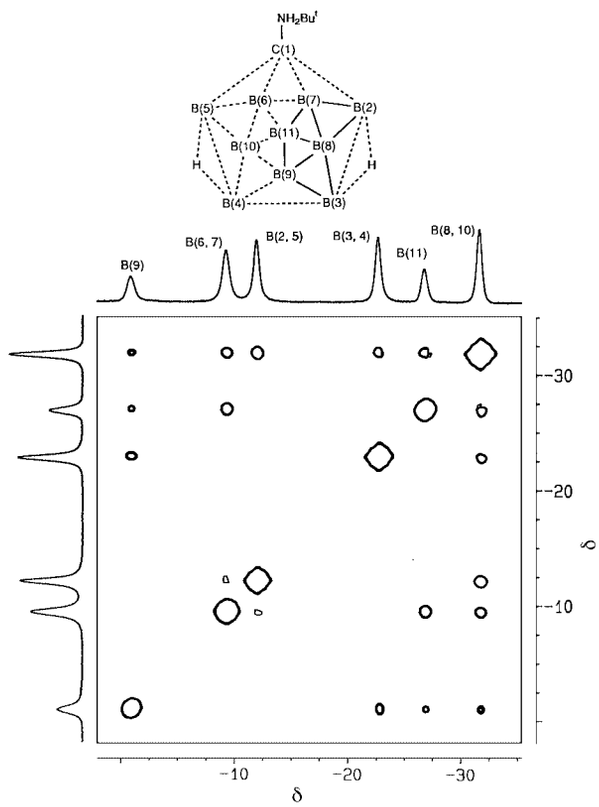


**Fig. 2** The $^{11}B$-{$^1H$}–$^{11}B$-{$^1H$} COSY 115.55 MHz NMR spectrum of compound **1**. The connectivity map employs the crystallographic numbering scheme, with terminal BH protons omitted for clarity

Based on structural parameters from the X-ray analysis, the LUMO (lowest unoccupied molecular orbital) was calculated for compound **1** using MOPAC, and is shown in Fig. 3. The

**Table 3** Selected internuclear distances (Å) and angles (°) for $[NEt_3(CH_2Ph)][nido\text{-}7\text{-}NHBu^t\text{-}7\text{-}CB_{10}H_{12}]$ **2** with estimated standard deviations in parentheses

| | | | | | | | |
|---|---|---|---|---|---|---|---|
| C(1)–N(1) | 1.460(2) | C(1)–B(2) | 1.658(3) | C(1)–B(5) | 1.670(3) | C(1)–B(6) | 1.690(3) |
| C(1)–B(7) | 1.711(2 | B(2)–B(7) | 1.790(3) | B(2)–B(8) | 1.795(3) | B(2)–B(3) | 1.864(3) |
| B(2)–H(23) | 1.33(2) | B(3)–C(9) | 1.756(3) | B(3)–B(8) | 1.778(3) | B(3)–B(4) | 1.896(3) |
| B(3)–H(23) | 1.22(2) | B(4)–B(9) | 1.748(3) | B(4)–B(10) | 1.790(3) | B(4)–B(5) | 1.854(3) |
| B(4)–H(45) | 1.22(2) | B(5)–B(10) | 1.775(3) | B(5)–B(6) | 1.794(3) | B(5)–H(45) | 1.33(2) |
| B(6)–B(7) | 1.737(3) | B(6)–B(11) | 1.757(3) | B(6)–B(10) | 1.776(3) | B(7)–B(11) | 1.757(3) |
| B(7)–B(8) | 1.762(3) | B(8)–B(9) | 1.777(2) | B(8)–B(11) | 1.780(3) | B(9)–B(11) | 1.765(3) |
| B(9)–B(10) | 1.785(3) | B(10)–B(11) | 1.788(3) | N(1)–C(2) | 1.489(2) | N(1)–H(1) | 0.95(2) |
| C(2)–C(4) | 1.458(5) | C(2)–C(4′) | 1.493(10) | C(2)–C(5) | 1.503(5) | C(2)–C(3′) | 1.504(10) |
| C(2)–C(3) | 1.507(5) | C(2)–C(5′) | 1.524(12) | | | | |

| | | | | | |
|---|---|---|---|---|---|
| N(1)–C(1)–B(2) | 120.4(2) | N(1)–C(1)–B(5) | 120.34(14) | B(2)–C(1)–B(5) | 110.19(14) |
| N(1)–C(1)–B(6) | 114.81(14) | B(2)–C(1)–B(6) | 114.06(14) | B(5)–C(1)–B(6) | 64.53(12) |
| N(1)–C(1)–B(7) | 115.44(14) | B(2)–C(1)–B(7) | 64.16(11) | B(5)–C(1)–B(7) | 113.67(14) |
| B(6)–C(1)–B(7) | 61.41(11) | C(1)–N(1)–C(2) | 119.30(14) | C(1)–N(1)–H(1) | 109.2(14) |
| C(2)–N(1)–H(1) | 106.4(14) | C(4)–C(2)–N(1) | 114.5(2) | N(1)–C(2)–C(4′) | 113.6(5) |
| C(4)–C(2)–C(5) | 108.0(4) | N(1)–C(2)–C(5) | 106.8(2) | N(1)–C(2)–C(3′) | 116.2(4) |
| C(4′)–C(2)–C(3′) | 105.5(6) | C(4)–C(2)–C(3) | 114.6(5) | N(1)–C(2)–C(3) | 106.6(3) |
| C(5)–C(2)–C(3) | 105.7(4) | N(1)–C(2)–C(5′) | 107.4(6) | C(4′)–C(2)–C(5′) | 107.8(7) |
| C(3′)–C(2)–C(5′) | 105.8(7) | | | | |

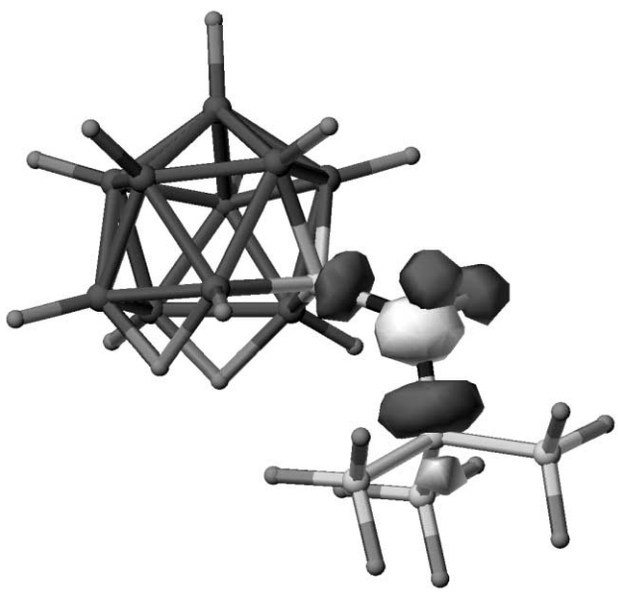

**Fig. 3** The result of the MOPAC calculation of the LUMO of compound **1**

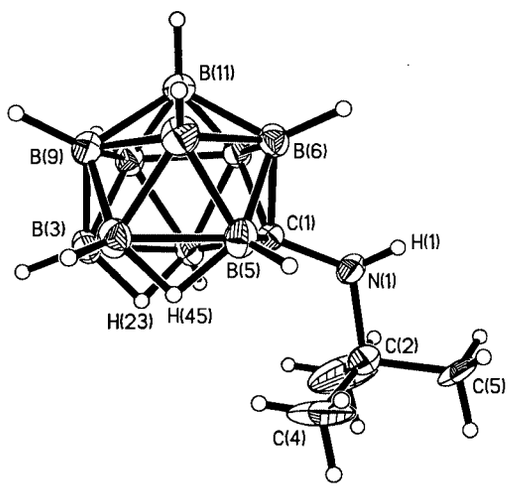


**Fig. 4** Molecular structure of the anion of $[NEt_3(CH_2Ph)][nido\text{-}7\text{-}NHBu^t\text{-}7\text{-}CB_{10}H_{12}]$ **2** showing the atom labelling scheme. Ellipsoids are drawn at the 40% probability level

LUMO is an antibonding orbital centred on the exopolyhedral nitrogen atom of the $NH_2Bu^t$ group and was shown to be relatively unaffected by torsional movement in the C–$NH_2Bu^t$ system. Its location suggests that the nitrogen atom would be susceptible to nucleophilic attack, and the notion of proton removal at this site is further supported by a frontier density analysis by the method of Fukui *et al.*[8] which shows the most likely site of attack by a nucleophile or base will be at the hydrogen atoms of the $NH_2Bu^t$ group, as opposed to the *endo*-B–H–B protons in the cage face.

Treatment of compound **1** with 1 equivalent of $LiBu^n$, followed by addition of $[NEt_3(CH_2Ph)]Cl$, gave the desired salt $[NEt_3(CH_2Ph)][nido\text{-}7\text{-}NHBu^t\text{-}7\text{-}CB_{10}H_{12}]$ **2**. Single crystals were obtained and the crystal structure determined (Fig. 4); selected internuclear distances and angles given in Table 3. The gross structural features are essentially similar to those of **1**. Moreover hydrogens H(23) and H(45), which bridge the connectivities B(2)–B(3) and B(4)–B(5), respectively, and the single NH hydrogen H(1) were all located and included in refinement. Thus the molecular orbital calculations predict initial deprotonation at the *exo*-nitrogen of **1**, and the X-ray analysis confirms this deprotonated species as the stable product **2**.

The conversion of the nitrogen from a quaternary into a tertiary centre is not sufficient to lower the symmetry of the system in solution, owing to rapid inversion at the nitrogen. Thus the $^{11}B\text{-}\{^1H\}$ NMR spectrum of compound **2** is similar in appearance to that of **1**, with peaks simply shifted to lower frequency. The signals were assigned (see Experimental section) from the $^{11}B\text{-}\{^1H\}$–$^{11}B\text{-}\{^1H\}$ COSY NMR spectrum (Fig. 5), which is almost identical in appearance to that of **1**. It is noteworthy, however, that the B(2, 5) ⟷ B(6, 7) correlation, while still weaker than those of the remaining peaks, is not as comparatively weak as that for compound **1**. This corresponds with slightly shorter internuclear distances for B(2)–B(7) [1.790(3)] and B(5)–B(6) [1.794(3) Å] observed in the structure of **2** as compared with those in **1** [1.813(3) and 1.812(3) Å, respectively]. This effect may be tentatively attributable to donation of some electron density from the nitrogen lone pair onto the cage-carbon atom. Indeed, in moving from compound **1** to **2**, a decrease of the C(1)–N(1) bond length from 1.508(2) to 1.460(2) Å is noted. However, this may be accounted for by a simple increase in trigonal $sp^2$ character of the nitrogen atom and unfortunately simple computational analysis on this aspect has proven inconclusive. The $^1H$ NMR spectrum of **2** displayed the usual broad peak at δ −4.20 for the *endo*-B–H–B protons and a singlet at δ 0.80 for the $Bu^t$ methyl protons. The NH proton resonance appeared at δ 4.00, this chemical shift being characteristic for this group and coming much further upfield

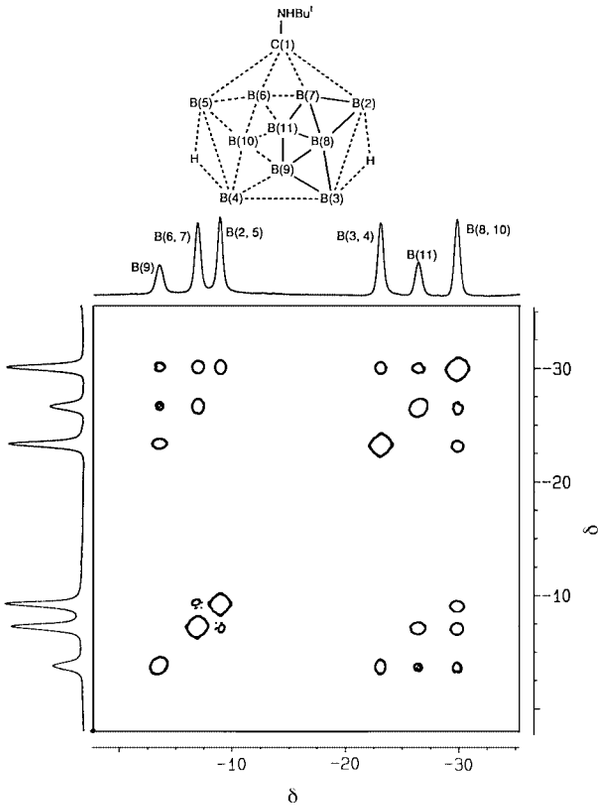


**Fig. 5** The $^{11}$B-{$^1$H}–$^{11}$B-{$^1$H} COSY 115.55 MHz NMR spectrum of compound **2**. Details as in Fig. 2

than that for the N$H_2$Bu$^t$ chemical shifts.[2b] The relative intensity of these three diagnostic signals in the $^1$H NMR spectrum is 2 : 9 : 1, respectively. The $^{13}$C-{$^1$H} NMR spectrum of **2** revealed a resonance at δ 68.7 for the cage-carbon nucleus, which is markedly shifted upfield by comparison with that of compound **1** (δ 93.1). The reason for this is uncertain, for although a shift in charge density about the carbon nucleus may be a contributing factor, as yet unidentified through-space effects may also be operating.

While monodeprotonation was the key process to investigate with regard to our metallacarbaborane work,[2] studies on the removal of a further proton from compound **2** were also of interest to us. The LUMO for **2** was again calculated using MOPAC (Fig. 6), employing X-ray structural parameters. This, coupled with a frontier density analysis,[8] strongly indicated that proton removal from the anion of **2** should occur at the cage face, *i.e.* displacement of one of the *endo*-B–H–B protons, and not the *exo*-nitrogen atom. However, attempts to form the dianion by treating tetrahydrofuran (thf) solutions of the $Li^+$ salt of **2** with LiBu$^n$ or NaH were difficult to monitor by NMR spectroscopy, as the desired species is extremely reactive, readily reacting with water from any source. An *in situ* experiment in an NMR tube contained within a Schlenk vessel proved partially successful, when a [$^2H_8$]thf solution of the $Li^+$ salt of **2** was treated with a slight excess of LiBu$^n$ and agitated for *ca.* 12 h. A $^{11}$B-{$^1$H} NMR spectrum revealed new and distinct high-field peaks at δ −12.7, −17.4, −21.5 and −39.2, almost certainly due to the dianionic cage. It was impossible to convert completely into the dianion under these conditions, and partial reversion to **2** was observed over a relatively short period of time (<1 h after removing the NMR tube from a nitrogen atmosphere), accompanied by the formation of small amounts of unidentified decomposition products. Despite the lack of diagnostic data, we are confident that the formula for the dianion can be written as *nido*-7-NHBu$^t$-7-$CB_{10}H_{11}^{2-}$ **3** as depicted in Scheme 1.

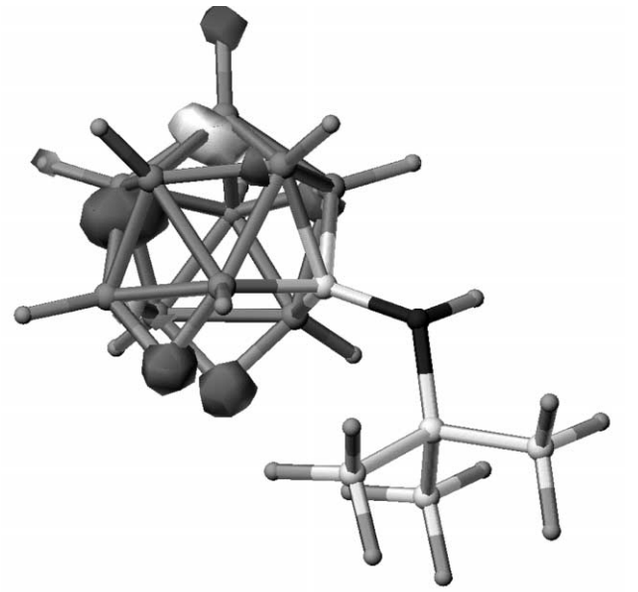

**Fig. 6** The result of the MOPAC calculation of the LUMO of compound **2**

With regard to successive deprotonations of the zwitterionic species **1** and the neutral dicarbaboranes *nido*-7,8-$R_2$-7,8-$C_2B_9H_{11}$ (R = H or Me), a fundamental difference in reactivity is noticed (Scheme 1). Clearly, the deprotonation of **1** does not proceed along a path where the anionic species produced would be isolobally related to the established deprotonation products of *nido*-7,8-$R_2$-7,8-$C_2B_9H_{11}$. We believe this behaviour has manifested itself in the novel results observed in our rhodacarbaborane chemistry.

## Conclusion

The facile deprotonation of compound **1** to give a stable monoanion provides a result consistent with our work on the metalla-co-ordinated species. Thus, we have found that the presence of the exopolyhedral $NH_2Bu^t$ group in **1** clearly adds an extra dimension to the chemistry of both the free cage species and the co-ordinated systems of derived metallacarbaboranes. Consequently there is scope for further investigation of low-valent transition-metal systems incorporating this type of monocarbaborane.

## Experimental

### General

All experiments were conducted under an atmosphere of dry nitrogen using Schlenk-tube techniques. Solvents were freshly distilled under nitrogen from appropriate drying agents before use. Decaborane was freshly sublimed before use. The NMR measurements were recorded at the following frequencies: $^1$H at 360.13, $^{13}$C at 90.56, $^{11}$B at 115.55 MHz. The $^{11}$B-{$^1$H} chemical shifts are positive to high frequency of $BF_3$·$Et_2O$ (external). The $^{11}$B-{$^1$H}–$^{11}$B-{$^1$H} COSY NMR spectrum of compound **1** in [$^2H_6$]acetone required a 512 × 512 point spectral matrix, with 32 transients per 512 time-domain points, giving an accumulation time of *ca.* 15 min in total. For the transformation, sine-bell and double sine-bell window functions were used for the f1 and f2 dimensions, respectively. A similar procedure was used for the $^{11}$B-{$^1$H}–$^{11}$B-{$^1$H} COSY NMR spectrum of compound **2**.

### Preparations

***nido*-7-$NH_2Bu^t$-7-$CB_{10}H_{12}$.** The carbaborane *nido*-7-$NH_2Bu^t$-7-$CB_{10}H_{12}$ was prepared by a modification of the procedure described previously for the species *nido*-7-$NH_2$R-7-$CB_{10}H_{12}$ (R = alkyl).[9] A 500 cm$^3$ three-neck flask, fitted with a pressure-

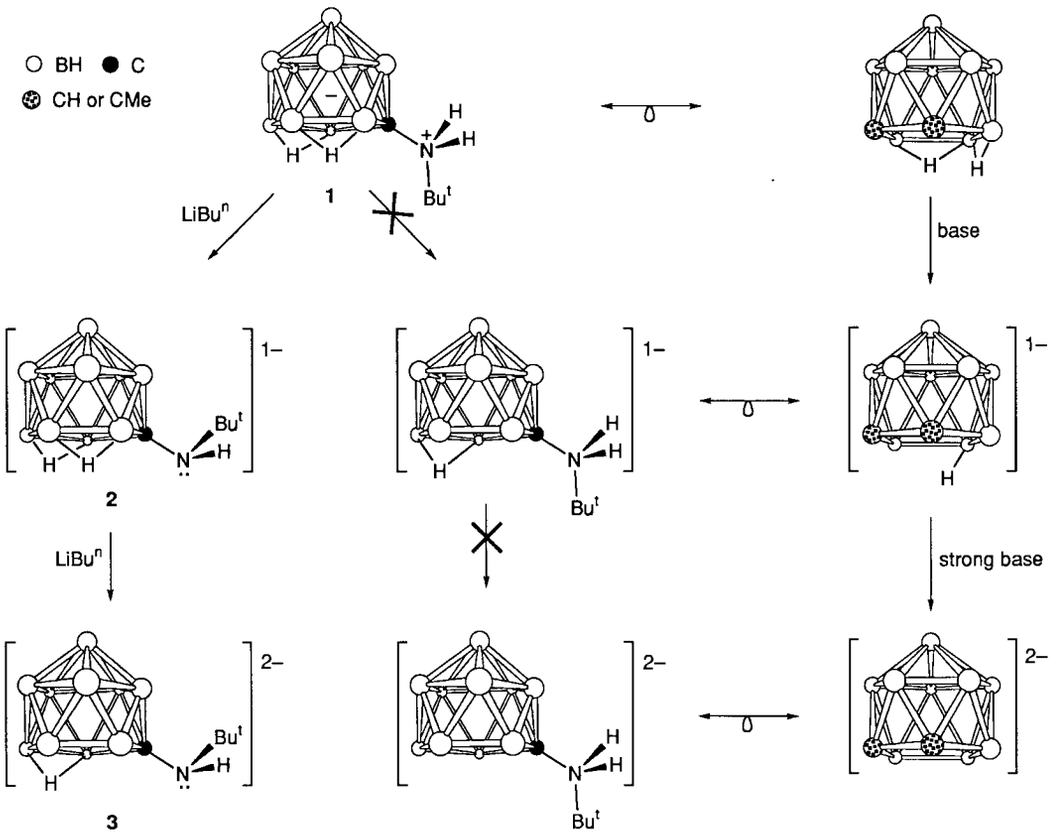


**Scheme 1** Reaction paths in the deprotonation of compounds **1** and *nido*-7,8-$R_2$-7,8-$C_2B_9H_{11}$ (R = H or Me). The location of the *endo*-B–H–B proton in **3** was taken from a structure-minimisation calculation by MOPAC

equalising dropping funnel and a condenser, was charged with decaborane (5.60 g, 0.046 mol) and dry benzene (200 $cm^3$). A solution of $CNBu^t$ (5.00 g, 0.06 mol) in benzene (10 $cm^3$) was added dropwise over a period of 15–20 min, and the mixture was refluxed for 3 h. The solid formed was removed by filtration, and washed with benzene (50 $cm^3$) to give *nido*-7-$NH_2Bu^t$-7-$CB_{10}H_{12}$ **1** (6.71 g, 90%), crystallised from hot ethanol–water (1:1, 8 $cm^3$) (Found: C, 29.3; H, 10.4; N, 6.7. $C_5H_{23}B_{10}N$ requires C, 29.2; H, 11.3; N, 6.8%). NMR ([$^2H_6$]-acetone): $\delta_H$ −3.62 (vbr, 2 H, B–H–B), 1.56 (s, 9 H, $Bu^t$) and 7.72 (s br, 2 H, $NH_2$); $\delta_C$ 93.1 (cage C), 64.1 ($CMe_3$) and 28.0 ($CMe_3$); $\delta_B$ −0.9 [1 B, B(9)], −9.4 [2 B, B(6), B(7)], −12.0 [2 B, B(2), B(5)], −22.8 [2 B, B(3), B(4)], −26.8 [1 B, B(11)] and −31.7 [2 B, B(8), B(10)].

**Deprotonation of *nido*-7-$NH_2Bu^t$-7-$CB_{10}H_{12}$.** A sample of compound **1** (0.20 g, 0.97 mmol) in thf (5 $cm^3$) was treated with $LiBu^n$ (0.50 $cm^3$, 1.00 mmol, 2.0 mol $dm^{-3}$ solution in cyclohexane) and the mixture was stirred for 2 h. The salt [$NEt_3(CH_2Ph)$]Cl (0.22 g, 0.97 mmol) was added and stirring continued (12 h) after which solvent was removed *in vacuo*. To the residue was added $CH_2Cl_2$ (20 $cm^3$) and the suspension filtered through Celite to remove LiCl. Solvent was then removed from the filtrate *in vacuo* and the residue crystallised from hot ethanol–water (1:1, 4 $cm^3$) to give *microcrystals* of [$NEt_3$-($CH_2Ph$)][*nido*-7-$NHBu^t$-7-$CB_{10}H_{12}$] **2** (0.32 g, 82%) (Found: C, 54.4; H, 10.8; N, 7.1. $C_{18}H_{44}B_{10}N_2$ requires C, 54.5; H, 11.2; N, 7.1%). NMR ([$^2H_6$]acetone): $\delta_H$ −4.20 (vbr, 2 H, B–H–B), 0.80 (s, 9 H, $Bu^t$), 1.06 [t br, 9 H, $CH_2Me$, *J*(HH) 7], 2.96 [q br, 9 H, $CH_2Me$, *J*(HH) 7 Hz], 4.00 (s br, 1 H, NH), 4.18 (s, 2 H, $CH_2Ph$) and 7.07–7.17 (m, 5 H, Ph); $\delta_C$ 133.3, 131.3, 130.0, 128.2 (Ph), 68.7 (cage C), 61.0 ($CH_2Ph$), 57.6 ($CMe_3$), 53.3 ($CH_2Me$), 30.4 ($CMe_3$) and 8.0 ($CH_2Me$); $\delta_B$ −3.5 [1 B, B(9)], −8.9 [2 B, B(6) and B(7)], −11.2 [2 B, B(2) and B(5)], −24.0 [2 B, B(3) and B(4)], −29.9 [1 B, B(11)] and −31.6 [2 B, B(8) and B(10)].

## Crystallography

Crystals of compounds **1** and **2** were grown from ethanol–water (1:1) mixtures. Data for **1** were collected at ambient temperatures using a Nicolet *P*3 four-circle diffractometer (Mo-Kα X-radiation, graphite monochromator, λ = 0.710 73 Å) with the crystal sealed under nitrogen in a capillary tube. Corrections for Lorentz-polarisation and X-ray absorption effects, the latter by an empirical method, were based upon azimuthal scan data.[10] A low-temperature data set for **2**, mounted on a glass fibre, was collected on a Siemens SMART CCD area-detector three-circle diffractometer (Mo-Kα X-radiation, λ = 0.710 73 Å). For three settings of φ, narrow data 'frames' were collected for 0.3° increments in ω. In this case 1321 frames of data were collected affording rather more than a hemisphere of data. The substantial redundancy in data allowed an empirical absorption correction to be applied using multiple measurements of equivalent reflections. Data frames were collected for 20 s per frame giving an overall data collection time of *ca.* 10 h. The frames were then integrated using SAINT.[10] Both structures were solved by conventional direct methods procedures and refined by full-matrix least squares on all $F^2$ data using SHELXTL[10] with anisotropic thermal parameters for all non-hydrogen atoms. For **1** the $NH_2$ and *endo*-B–H–B protons were located from final electron-density difference syntheses and their positions were refined. The terminal BH and Me protons were included in calculated positions and allowed to ride on the parent boron or carbon atoms with isotropic thermal parameters [$U_{iso}$ = $1.2U_{iso\ (equiv)}$ of the parent atom except for Me protons where $U_{iso} = 1.5U_{iso\ (equiv)}$] with refined B–H and C–H distances. For **2** the NH and *endo*-B–H–B protons were located from final electron-density difference syntheses and included in the refinement. All terminal BH protons were also located and refined. The methyl, methylene and phenyl protons of the cation were included in calculated positions and allowed to ride on their parent carbon atoms with isotropic thermal parameters

**Table 4.** Crystallographic data for compounds **1** and **2**

| | **1** | **2** |
|---|---|---|
| Chemical formula | $C_5H_{23}B_{10}N$ | $C_{18}H_{44}B_{10}N_2$ |
| *M* | 205.34 | 396.65 |
| *T*/K | 293 | 173 |
| Colour, habit | White plate | White prism |
| Crystal size/mm | 0.20 × 0.60 × 0.70 | 0.40 × 0.45 × 0.70 |
| Crystal system | Orthorhombic | Monoclinic |
| Space group | *Pbca* | $P2_1/n$ |
| *a*/Å | 10.507(5) | 10.651(2) |
| *b*/Å | 13.805(6) | 11.652(2) |
| *c*/Å | 18.093(9) | 20.926(3) |
| β/° | — | 101.77(2) |
| *U*/Å$^3$ | 2624(2) | 2542.5(8) |
| *Z* | 8 | 4 |
| $D_c$/g cm$^{-3}$ | 1.039 | 1.036 |
| μ(Mo-Kα)/mm$^{-1}$ | 0.048 | 0.053 |
| *F*(000) | 880 | 864 |
| No. reflections collected | 2312 | 11 763 |
| No. independent reflections | 2312 | 4461 |
| 2θ Range/° | 5.0–50.0 | 4.7–50.1 |
| Final residuals *wR2*,[a] *R1*[b] | 0.139, 0.051 | 0.145, 0.054 |
| Weighting factors a,b | 0.0644, 0.8994 | 0.0614, 1.2617 |
| Goodness of fit on $F^2$ | 1.035 | 1.064 |
| Largest difference peak, hole/e Å$^{-3}$ | 0.17, −0.16 | 0.23, −0.28 |

[a] Structure was refined on $F_o^2$ using all data: $wR2 = [\Sigma w(F_o^2 - F_c^2)^2/\Sigma w(F_o^2)^2]^{\frac{1}{2}}$ where $w^{-1} = [\sigma^2(F_o^2) + (aP)^2 + bP]$ and $P = [\max(F_o^2,0) + 2F_c^2]/3$. [b] The value is given for comparison with refinements based on $F_o$ with a typical threshold of $F_o > 4\sigma(F_o)$, $R1 = \Sigma||F_o| - |F_c||/\Sigma|F_o|$ and $w^{-1} = [\sigma^2(F_o) + gF_o^2]$. The numbers of independent reflections which satisfy $F_o > 4\sigma(F_o)$ are 1694 (**1**) and 3671 (**2**).

[$U_{iso} = 1.2U_{iso\ (equiv)}$ of the parent atom except for Me protons where $U_{iso} = 1.5U_{iso\ (equiv)}$]. The Bu$^t$ methyl groups were found to be disordered over two sites and were not stable in refinement. After site-occupancy refinement the disordered components were assigned fixed site-occupation factors of 0.71 and 0.29 and were restrained to have similar bond lengths and angles. The Bu$^t$ methyl protons were included in calculated positions with isotropic thermal parameters [$U_{iso} = 1.5U_{iso\ (equiv)}$ of the parent carbon atoms]. They were accorded the appropriate site-occupancy factors of their parent carbon atoms but not allowed to ride on them. Crystallographic data for both structures are listed in Table 4. All calculations were carried out on Silicon Graphics Iris, Indigo or Indy computers.

Atomic coordinates, thermal parameters, and bond lengths and angles have been deposited at the Cambridge Crystallographic Data Centre (CCDC). See Instructions for Authors, *J. Chem. Soc.*, *Dalton Trans.* 1997, Issue 1. Any request to the CCDC for this material should quote the full literature citation and the reference number 186/389.

### Molecular orbital calculations

All calculations were carried out using MOPAC[5] with AM1 parameters. The geometries for compounds **1** and **2** were obtained from the single-crystal structure determinations reported in this paper. To test the utility of MOPAC for modelling the monocarbaborane systems, full geometry minimisations were also carried out and the resulting structures were in good agreement with those obtained from the crystallographic studies.

## Acknowledgements

We thank the Robert A. Welch Foundation for support (Grant AA-1201).

## References

1 D. E. Hyatt, D. A. Owen and L. J. Todd, *Inorg. Chem.*, 1966, **5**, 1749.
2 (*a*) V. N. Lebedev, D. F. Mullica, E. L. Sappenfield and F. G. A. Stone, *Organometallics*, 1996, **15**, 1669; (*b*) J. C. Jeffery, V. N. Lebedev and F. G. A. Stone, *Inorg. Chem.*, 1996, **35**, 2967; (*c*) J. C. Jeffery, P. A. Jelliss, V. N. Lebedev and F. G. A. Stone, *Organometallics*, 1996, **15**, 4737; (*d*) V. N. Lebedev, D. F. Mullica, E. L. Sappenfield and F. G. A. Stone, *J. Organomet. Chem.*, 1997, in the press.
3 T. L. Venable, W. C. Hutton and R. N. Grimes, *J. Am. Chem. Soc.*, 1984, **106**, 29.
4 (*a*) O. W. Howarth, M. J. Jasztal, J. G. Taylor and M. G. H. Wallbridge, *Polyhedron*, 1985, **4**, 1461; (*b*) A. E. Wille, J. Plešek, J. Holub, B. Štíbr, P. J. Carroll and L. G. Sneddon, *Inorg. Chem.*, 1996, **35**, 5342.
5 MOPAC, Version 94, CAChe Scientific, The Oxford Molecular Group, Oxford, 1994.
6 (*a*) T. Onak, in *Comprehensive Organometallic Chemistry II*, eds.-in-chief E. W. Abel, F. G. A. Stone and G. Wilkinson, Pergamon (Elsevier), Oxford, 1995, vol. 1 (ed. C. E. Housecroft), sect. 6; (*b*) M. F. Hawthorne, T. D. Andrews, P. M. Garrett, F. P. Olsen, M. Reintjes, F. N. Tebbe, L. F. Warren, P. A. Wegner and D. C. Young, *Inorg. Synth.*, 1967, **10**, 91; (*c*) J. Buchanan, E. J. M. Hamilton, D. Reed and A. J. Welch, *J. Chem. Soc.*, *Dalton Trans.*, 1990, 677.
7 R. N. Grimes, in *Comprehensive Organometallic Chemistry II*, eds.-in-chief E. W. Abel, F. G. A. Stone and G. Wilkinson, Pergamon (Elsevier), Oxford, 1995, vol. 1 (ed. C. E. Housecroft), sect. 9.
8 K. Fukui, T. Yonezawa, C. Nagata and H. Shingu, *J. Chem. Phys.*, 1953, **11**, 1433.
9 W. H. Noth, J. L. Little, J. R. Lawrence, F. R. Scholer and L. J. Todd, *Inorg. Synth.*, 1968, **11**, 33.
10 SHELXTL, version 5.03, Siemens X-Ray Instruments, Madison, WI, 1995.

*Received* 22*nd October* 1996; *Paper* 6/07212G